

Ferrocenyl–Naphthalimide Donor–Acceptor Dyads with Aromatic Spacer Groups

C. John McAdam, Brian H. Robinson, Jim Simpson,* and Tei Tagg

Department of Chemistry, University of Otago, P.O. Box 56, Dunedin 9054, New Zealand.

Received January 20, 2010

The preparation and characterization of a series of dyads containing ferrocene donor and naphthalimide acceptor units, separated by aromatic spacer groups, are reported. The compounds contain a ferrocene-ethynyl spacer component linked to the 4-position of a naphthalimide by an ethynyl bridge, Fc–CH=CH–spacer–C≡C–naphthalimide (Fc = ferrocenyl), where the spacers are 1,4-phenyl, 4,4'-biphenyl, and 9,10-anthryl. Precursors to the dyad systems, halo-spacer–C≡C–naphthalimide, are also characterized where the halo-spacers are 1-bromophenyl, 4-bromobiphenyl, and 9-iodoanthryl. Various synthetic strategies are examined, with attachment of the spacer to 4-ethynyl-naphthalimide followed by reaction with ethynylferrocene proving the most effective route. Crystal structures of the donor–spacer–acceptor (D–S–A) compound (*E*)-1-ethynylferrocenyl-4-(4-ethynyl-*N*-methyl-1,8-naphthalimide)benzene (**7**) and the precursor compounds (*E*)-4-bromo-4'-(ethynylferrocenyl)biphenyl (**2**) and 4-ethynyl-4'-(4-ethynyl-*N*-methyl-1,8-naphthalimide)biphenyl (**4**) are reported, with packing in the two naphthalimide derivatives dominated by offset π -stacking interactions. Compounds containing the ferrocenyl groups show the anticipated one-electron oxidation processes at potentials that vary little with the spacer groups. Both the ferrocenyl derivatives and their naphthalimide precursors show reversible reduction waves. The single wave for the phenyl and biphenyl compounds and their precursors is assigned to reversible one-electron reduction of the naphthalimide unit. The corresponding anthracene derivatives display two reversible reductions associated with the naphthalimide and the anthryl moieties, respectively.

Introduction

Ferrocene compounds continue to attract attention due to their combination of electronic and robust physical properties.¹ Research contributions cover a wealth of disciplines,

from biological to material science applications, and with outputs that range from esoteric to practical and commercial in nature.² One area of particular activity is the study of nonlinear optical (NLO) behavior³ of donor–acceptor (D–A) dyads. The ferrocenyl moiety has proven to be readily incorporated (in a donor role) into push–pull assemblies, generally in conjunction with connective links comprising single or multiple π -systems.⁴

We have recently investigated the preparation and spectroscopic and electrochemical properties of simple ferrocene dyads with alkene or alkyne links. Acceptors include polyaromatics,⁵ acridone and anthraquinone,⁶ and importantly in the context of this work, model 1,8-naphthalimide systems (Figure 1)⁷ and related naphthalic anhydrides.^{7,8} In all cases, there was strong evidence not only for charge separation in the excited states of the molecules but also for a reversal of the donor–acceptor roles upon the one-electron oxidation of the ferrocene. This is signaled by the appearance of strongly solvatochromic LMCT transitions⁹ in the near-IR. Absorption

*Corresponding author. E-mail: jsimpson@alkali.otago.ac.nz.

(1) Togni, A.; Hayashi, T. *Ferrocenes*; VCH: Weinheim, Germany, 1995.

(2) (a) Wang, J. *Chem. Rev.* **2008**, *108*, 814. (b) Szacilowski, K. *Chem. Rev.* **2008**, *108*, 3481. (c) Whittell, G. R.; Manners, I. *Adv. Mater.* **2007**, *19*, 3439.

(3) (a) Marder, S. R. *Inorganic Materials*, 2nd ed.; Bruce, D. W.; O'Hare, D., Eds.; Wiley: Chichester, 1996. (b) Long, N. J. *Angew. Chem., Int. Ed. Engl.* **1995**, *34*, 21.

(4) (a) Barlow, S.; Bunting, H. E.; Ringham, C.; Green, J. C.; Bublitz, G. U.; Boxer, S. G.; Perry, J. W.; Marder, S. R. *J. Am. Chem. Soc.* **1999**, *121*, 3715. (b) Jayaprakash, K. N.; Ray, P. C.; Matsuoka, I.; Bhadbhade, M. M.; Puranik, V. G.; Das, P. K.; Nishihara, H.; Sarkar, A. *Organometallics* **1999**, *18*, 3851. (c) Hudson, R. D. A.; Asselberghs, I.; Clays, K.; Cuffe, L. P.; Gallagher, J. F.; Manning, A. R.; Persoons, A.; Wostyn, K. *J. Organomet. Chem.* **2001**, *637–639*, 435. (d) Mata, J. A.; Peris, E.; Llusar, R.; Uriel, S.; Cifuentes, M. P.; Humphrey, M. G.; Samoc, M.; Luther-Davies, B. *Eur. J. Inorg. Chem.* **2001**, 2113. (e) Malaun, M.; Kowallick, R.; McDonagh, A. M.; Marcaccio, M.; Paul, R. L.; Asselberghs, I.; Clays, K.; Persoons, A.; Bildstein, B.; Fiorini, C.; Nunzi, J.-M.; Ward, M. D.; McCleverty, J. A. *J. Chem. Soc., Dalton Trans.* **2001**, 3025. (f) Mueller-Westerhoff, U. T.; Sanders, R. W. *Organometallics* **2003**, *22*, 4778. (g) Zhang, F.; Vill, V.; Heck, J. *Organometallics* **2004**, *23*, 3853. (h) Colbran, S. B.; Lee, S. T.; Donnon, D. G.; Maharaj, F. J. D.; McDonagh, A. M.; Walker, K. A.; Young, R. D. *Organometallics* **2006**, *25*, 2216. (i) Winters, M. U.; Dahlstedt, E.; Blades, H. E.; Wilson, C. J.; Frampton, M. J.; Anderson, H. L.; Albinsson, B. *J. Am. Chem. Soc.* **2007**, *129*, 4291. (j) Kinnibrugh, T. L.; Salman, S.; Getmanenko, Y. A.; Coropceanu, V.; Porter, W. W., III; Timofeeva, T. V.; Matzger, A. J.; Brédas, J.-L.; Marder, S. R.; Barlow, S. *Organometallics* **2009**, *28*, 1350.

(5) Cuffe, L.; Hudson, R. D. A.; Gallagher, J. F.; Jennings, S.; McAdam, C. J.; Connelly, R. B. T.; Manning, A. R.; Robinson, B. H.; Simpson, J. *Organometallics* **2005**, *24*, 2051.

(6) McGale, E. M.; Robinson, B. H.; Simpson, J. *Organometallics* **2003**, *22*, 931.

(7) McAdam, C. J.; Morgan, J. L.; Robinson, B. H.; Simpson, J.; Rieger, P. H.; Rieger, A. L. *Organometallics* **2003**, *22*, 5126.

(8) Munro, N. H.; Hanton, L. R.; McAdam, C. J.; McMorran, D. A. *Acta Crystallogr.* **2008**, *E64*, m572.

(9) Flood, A. H.; McAdam, C. J.; Gordon, K. C.; Kjaergaard, H. G.; Manning, A. R.; Robinson, B. H.; Simpson, J. *Polyhedron* **2007**, *26*, 448.

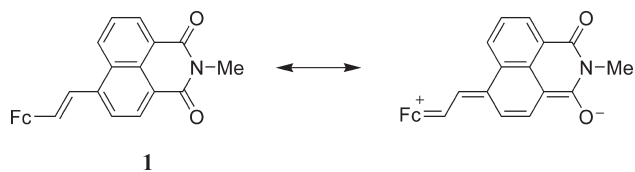


Figure 1. Ferrocenyl naphthalimide dyad **1** and representation of the charge transfer excited state.

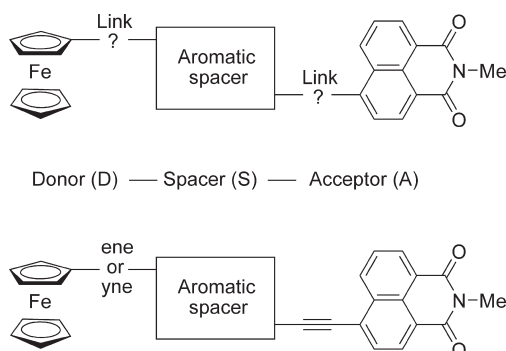
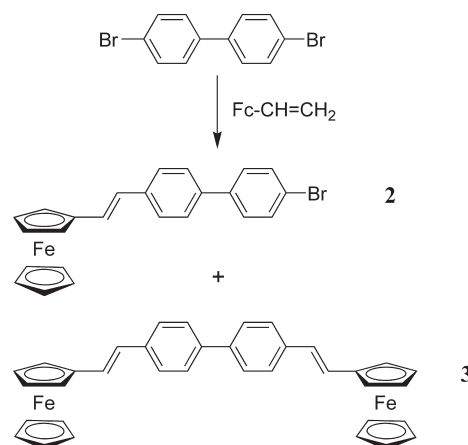


Figure 2. Generic (upper) and target (lower) D–S–A assemblies.

of NIR radiation has attracted considerable recent attention due to the potential applications in both telecommunications and for *in vivo* luminescent imaging.¹⁰ Similar behavior is also observed for ferrocenyl–cobalt metallocene dyads,¹¹ and naphthalimide,¹² or polyaromatic acceptor systems¹³ where the ferrocenyl moiety is replaced by metal acetylides from groups 8 and 10. This charge separation is critically dependent on the link between the donor and acceptor systems with $C=C-C=C > C=C > C\equiv C$ for a given donor–acceptor combination.

Our selection of the 4-naphthalimido moiety for the acceptor role in D–A dyads is attractive for several reasons; first, is its strength as an acceptor, on a par with *p*-nitrophenyl.¹² Additionally, synthesis of 4-substituted naphthalimides is facilitated by the ready availability of 4-bromonaphthalic anhydride starting material and a well-characterized¹⁴ and high-yielding derivative chemistry. Ultimately, these naphthalimides offer the tantalizing possibility of multiresponsive electro- and photoactive species. In sharply contrasting behavior, spectral properties are much less affected in situations where the redox-active ferrocene unit is located in the *N*-headgroup of the naphthalimide due to the existence of a node at the imide nitrogen. In such cases, photophysical characteristics of the molecules appear to be dependent on

Scheme 1



through-space interactions between the excited state of the naphthalimide and the ferrocenyl headgroup.^{7,15}

It is on these premises that we examine here synthetic routes to interpolate an additional aromatic spacer between the donor and acceptor units of **1** and the resulting effect on the spectroscopic and electrochemical behavior of the materials formed.

Results and Discussion

The interpolation of an aromatic spacer into a ferrocenyl–naphthalimide D–A compound like **1** to prepare donor–spacer–acceptor (D–S–A) assemblies [Figure 2 (upper)] can potentially be approached from either terminus or constructed outward from the central spacer. Upon considering connective links (direct attachment, alkyne link, alkene link, polyene link, etc.), a bewildering number of permutations and synthetic strategies arises. To limit these, we determined to focus on 4-ethynyl-naphthalimides, Figure 2 (lower).

Our first strategy was to prepare monoferrocenyl-substituted derivatives (D–S–X) of the desired dihalogenated aromatic spacer (X–S–X) via Heck or Sonogashira coupling. This would then be reacted with 4-ethynyl-naphthalimide to generate the D–S–A assembly.

This approach, Scheme 1, was used to prepare 4-bromo-4'-(ethynylferrocenyl)biphenyl, **2**. Ethynylferrocene was reacted with an equimolar quantity of 4,4'-dibromobiphenyl under Heck coupling conditions.¹⁶ The yield however was poor, the major product being the disubstituted 4,4'-bis(ethynylferrocenyl)biphenyl (**3**).¹⁷ Sufficient quantities of **2** for an X-ray crystallographic study and characterization purposes were obtained, but the practical difficulties of separation of minor from major reaction components led us to explore alternative synthetic strategies.

Our next approach was to couple the ferrocenyl donor with a preprepared spacer–naphthalimide component as depicted, again with the biphenyl group, in Scheme 2. Desilylation of 4,4'-bis(trimethylsilylethynyl)biphenyl followed by reaction with an equimolar quantity of 4-bromo-*N*-methyl-1,8-naphthalimide under Sonogashira conditions¹⁸ gave the

(10) (a) Wang, Z. Y.; Zhang, J.; Wu, X.; Birau, M.; Yu, G.; Yu, H.; Qi, Y.; Desjardins, P.; Meng, X.; Gao, J. P.; Todd, E.; Song, N.; Bai, Y.; Beaudin, A. M. R.; LeClair, G. *Pure Appl. Chem.* **2004**, *76*, 1435. (b) Ward, M. D. *Coord. Chem. Rev.* **2007**, *251*, 1663.

(11) Kjaergaard, H. G.; McAdam, C. J.; Manning, A. R.; Mueller-Bunz, H.; O'Donohue, P.; Ortin, Y.; Robinson, B. H.; Simpson, J. *Inorg. Chim. Acta* **2008**, *361*, 1616.

(12) McAdam, C. J.; Manning, A. R.; Robinson, B. H.; Simpson, J. *Inorg. Chim. Acta* **2005**, *358*, 1673.

(13) Butler, P.; Gallagher, J. F.; Manning, A. R.; Mueller-Bunz, H.; McAdam, C. J.; Robinson, B. H.; Simpson, J. *J. Organomet. Chem.* **2005**, *690*, 4545.

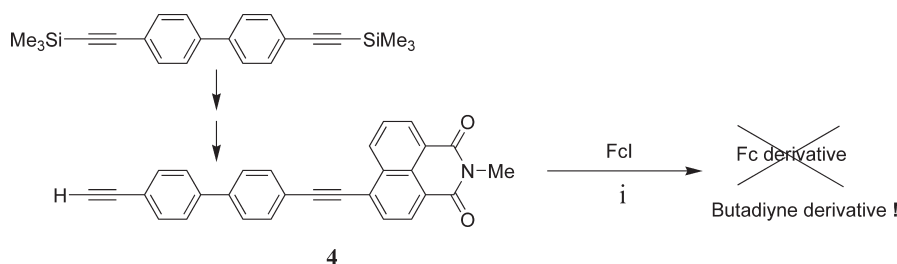
(14) (a) de Silva, A. P.; Gunaratne, H. Q. N.; Gunnaugsson, T.; Huxley, A. J. M.; McCoy, C. P.; Rademacher, J. T.; Rice, T. E. *Chem. Rev.* **1997**, *97*, 1515. (b) Wintgens, V.; Valat, P.; Kossanyi, J.; Biczok, L.; Demeter, A.; Berces, T. *J. Chem. Soc., Faraday Trans. 1* **1994**, *90*, 411. (c) Gan, J.; Tian, H.; Wang, Z.; Chen, K.; Hill, J.; Lane, P. A.; Rahn, M. D.; Fox, A. M.; Bradley, D. D. C. *J. Organomet. Chem.* **2002**, *645*, 168.

(15) McAdam, C. J.; Robinson, B. H.; Simpson, J. *Organometallics* **2000**, *19*, 3644.

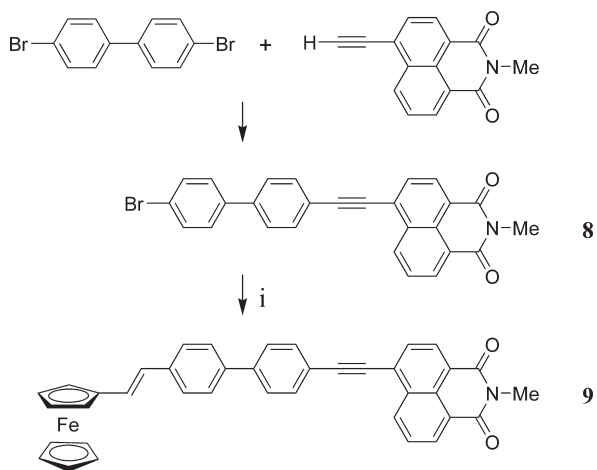
(16) Heck, R. F.; Nolley, J. P., Jr. *J. Org. Chem.* **1972**, *37*, 2320.

(17) Rodriguez, J.-G.; Mayo, M.; Fonseca, I. *J. Organomet. Chem.* **1997**, *534*, 35.

(18) Sonogashira, K.; Tohda, Y.; Hagihara, N. *Tetrahedron Lett.* **1975**, *16*, 4467.

Scheme 2^a

^a(i) Pd(Ph₃)₂Cl₂, CuI, ^tPr₂NH.

Scheme 3^a

^a(i) Fc-CH=CH₂, Pd(OAc)₂, (*o*-tolyl)₃P, Et₃N, DMF.

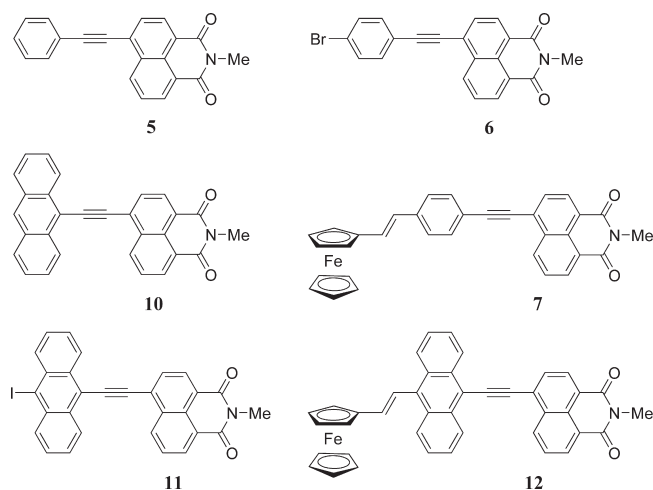
required product, **4**, in good yield, Scheme 2. However, attempts to cross couple **4** with iodoferrrocene were entirely unsuccessful due to oxidative coupling that produced the sparingly soluble and generally intractable bis[(naphthalimidoethynyl)biphenyl]buta-1,3-diyne as the major product.

A corresponding reaction scheme starting from 9,10-bis(trimethylsilyl)ethynylanthracene gave no anthryl equivalent of **4**, presumably due to the instability of the deprotected 9,10-diethynylantracene.

In the third and ultimately successful route, Sonogashira coupling of 4-ethynyl-*N*-methyl-1,8-naphthalimide with stoichiometric 4,4'-dibromobiphenyl gave the monocoupled bromobiphenyl derivative, **8**. Heck coupling of this halo-spacer-acceptor (X-S-A) **6** to ethynylferrocene gave the desired D-S-A system, **9** (Scheme 3).

The same two-step strategy was used to produce the haloaromatic X-S-A intermediates **6** and **11** and subsequently D-S-A molecules with 1,4-phenyl, **7**, and 9,10-anthryl, **12**, groups as spacers. The yields of the monoethynylated X-S-A were not high (15–25%), and undoubtedly, although not characterized, significant quantities of disubstituted A-S-A products were formed. Nevertheless isolation proved more successful, and ultimately fruitful, than the monoferrrocenylated D-S-X methodology (Scheme 1). To provide a clearer understanding of electrochemical and spectroscopic results, reference compounds **5** and **10** were similarly synthesized from iodobenzene and 9-bromoanthracene, respectively. Following on from, and complementary to, the ferrocenylethynyl D-S-A derivatives presented here, the preparation of a series of ferrocenylethynyl

D-S-A's and their attendant computational study will be reported on separately.¹⁹



All compounds were characterized by elemental analysis, MS, NMR, and electronic spectra. The 4-aryl-substituted naphthalimide derivatives are yellow and strongly fluorescent, the exceptions being **10** and **11**, which are red. The ferrocenyl D-S-A compounds are characteristically orange-red with no apparent fluorescence. The thermodynamically favored *E*-configuration for the alkene system of these derivatives (**2**, **3**, **7**, **9**, and **12**) is obtained without the need for additional *cis*-*trans* conversion⁵ and was established unambiguously by ¹H and 2-D NMR techniques, with additional confirmation in the case of **2** and **7** by X-ray crystallography. Compounds **2**–**12** are moderately to readily soluble in chlorinated solvents but poorly soluble in aromatic solvents and alcohols. This provided us with some challenges in obtaining crystals of sufficient quality for X-ray determinations, presumably due to ready aggregation in the solid state associated with π - π stacking interactions.¹⁵ Only intermediate molecules **2** and **4** and one complete D-S-A molecule, **7**, gave crystals suitable for X-ray crystallography. Their structures are reported here.

Crystal Structure of 2. The structure of **2** consists of a ferrocenyl group linked by a disordered alkene bridge to a 4,4'-biphenyl unit with a bromo-substituent in the 4'-position and one cyclopentadienyl ring of a ferrocene molecule in the 4-position, Figure 3.

The phenyl rings of the biphenyl are almost coplanar with a dihedral angle of 4.32(18)^o between them. The C7...C12

(19) Tagg, T.; Kjaergaard, H. G.; Lane, J. R.; McAdam, C. J.; Robinson, B. H.; Simpson, J. *Organometallics*, manuscript in preparation.

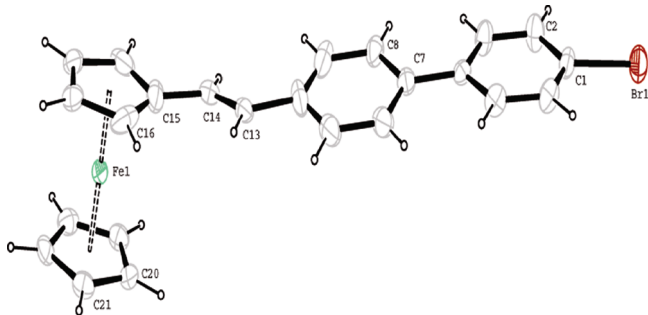


Figure 3. Structure of **2** showing the atom-numbering scheme with ellipsoids drawn at the 50% probability level. For clarity, only atoms of the major disorder component of the disordered alkene group are shown and only the first two C atoms of consecutively numbered phenyl and cyclopentadienyl rings are numbered. Selected bond distances [Å] and angles [deg]: C10–C13 1.506(7); C13–C14 1.309(10); C14–C15 1.509(7); C4–C7 1.490(4); C1–Br1 1.905(3); (C15···C19) ring av C–C 1.415(9); (C20···C24) ring av C–C 1.420(3); Fe1···(C15–C19) av 2.045(6); Fe1···(C20–C24) av 2.047(3); C10–C13–C14 122.0(6); C13–C14–C15 116.5(6).

phenyl ring makes an angle of 17.52(19)° to the substituted cyclopentadienyl ring of the ferrocene moiety. The C=C bond distances in the two disordered components of the linking alkene unit, 1.320(6) and 1.324(6) Å, are unremarkable.²⁰ A search of the Cambridge database (V 5.31 to November 2009)²¹ reveals 46 other *p*-substituted phenyl rings bound to alkene ferrocenyl groups; analysis of the C=C bonds in these molecules using Vista²² shows a mean C=C distance of 1.32(3) Å. The cyclopentadienyl rings of the ferrocene are staggered, with a mean Cm–Cg1–Cg2–Cn torsion angle of 25.7(4)° (Cg1 and Cg2 are the centroids of the cyclopentadienyl rings, *m* = 15–19 when *n* = 20–24), and the dihedral angle between the two Cp ring planes is 1.3(3)°.

The absence of a naphthalimide group in **2** lessens the opportunities for π -stacking interactions in this system. Not surprisingly therefore, crystal packing in the solid state structure of this molecule relies on nonclassical C–H···Br hydrogen bonds²³ and C–H··· π interactions that link the molecules into zigzag chains down the *b* axis (Supporting Information, Figure S1).

Crystal Structure of 4. The compound comprises an *N*-methyl-1,8-naphthalimide unit linked at the 4-position to a biphenyl group through an alkyne bridge, Figure 4. The biphenyl carries a terminal alkyne substituent in the 4'-position. The C28≡C29 bond of the terminal alkyne is significantly shorter, 1.146(2) Å, than that of C14≡C15, 1.201(2) Å, which links the naphthalimide and biphenyl systems. This and the relatively short C4–C14 and C15–C16 bonds, 1.4307(19) and 1.4323(19) Å, suggest some delocalization between the naphthalimide and the biphenyl systems.

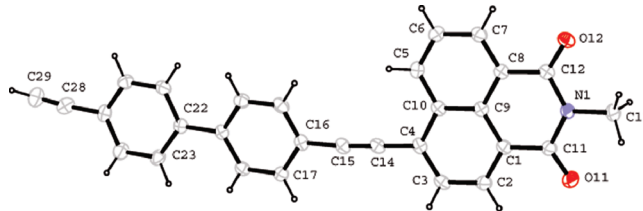


Figure 4. Structure of **4** showing the atom-numbering scheme with ellipsoids drawn at the 50% probability level. For clarity only the first two C atoms of consecutively numbered phenyl rings are numbered. Selected bond distances [Å] and angles [deg]: C4–C14 1.4307(19); C14–C15 1.201(2); C15–C16 1.423(19); C19–C22 1.4822(19); C25–C28 1.469(2); C28–C29 1.146(2); C4–C14–C15 179.94(19); C14–C15–C16 175.06(15); C25–C28–C29 175.10(18).

Bond lengths and angles in the naphthalenedicarboximide fragment compare well with those found in similar systems,^{7,12,15,24} with the bond lengths in the dicarboximide ring suggesting a degree of delocalization over the entire naphthalimide unit, but this does not extend to the methyl substituent on the N1 atom.²⁵ The naphthalimide unit is reasonably planar with an rms deviation of 0.0156 Å from the best fit mean plane and, importantly, makes an angle of just 6.80(6)° to the C16···C21 ring of the biphenyl moiety, again consistent with a highly desirable degree of delocalization between the spacer and acceptor components of this D–S–A intermediate. The two biphenyl rings are inclined to one another at an angle of 9.41(8)°.

In the crystal, C–H···O and C–H··· π interactions form zigzag chains along the *c* axis. Further C–H···O hydrogen bonds and, inevitably for a naphthalimide system, extensive π – π stacking interactions form stacks of parallel chains down *a* (Supporting Information, Figure S2).

Crystal Structure of 7. As detailed in the Experimental Section, there was positional disorder involving the alkyne group and the naphthalimide unit in this structure. In the discussion that follows, data will be discussed only for the major disorder component of the structure. The compound comprises a ferrocenyl linked from the cyclopentadiene ring by an *E*-configured alkene to a benzene ring. In the para-position of the benzene ring, an alkyne bridge connects to the 4-position of an *N*-methyl-1,8-naphthalimide, Figure 5. The molecule thus comprises a complete D–S–A system. One benzene solvate molecule completes the asymmetric unit of the compound.

The C14≡C15 bond (1.207(14) Å) of the alkyne is not unusual and compares with a distance of 1.201(2) Å in **4**. Similarly, the C22=C23 alkene bond at 1.318(12) Å compares well with the values found in **2** and in the other *p*-substituted phenyl rings bound to alkene ferrocenyl groups mentioned previously. The naphthalimide unit is again reasonably planar, with an rms deviation of 0.0183 Å from the best fit mean plane, and makes an angle of 3.1(4)° to the C16···C21 benzene ring. This in turn is inclined at an angle of 6.1(5)° to the substituted cyclopentadiene ring of the ferrocenyl moiety. The cyclopentadienyl rings of the ferrocene are approximately eclipsed, and the dihedral angle between the two Cp ring planes is 2.2(6)°.

(20) McAdam, C. J.; Robinson, B. H.; Simpson, J. *Inorg. Chim. Acta* **2008**, *361*, 2172.

(21) Allen, F. H. *Acta Crystallogr.* **2002**, *B58*, 380.

(22) Cambridge Crystallographic Data Centre. *Vista—A Program for the Analysis and Display of Data Retrieved from the CSD*; Cambridge Crystallographic Data Centre: Cambridge, England, 1994.

(23) (a) McAdam, C. J.; Robinson, B. H.; Simpson, J. *Acta Crystallogr.* **2007**, *E63*, m1362. (b) Tagg, T.; McAdam, C. J.; Robinson, B. H.; Simpson, J. *Acta Crystallogr.* **2008**, *C64*, o388. (c) McAdam, C. J.; Hanton, L. R.; Moratti, S. C.; Simpson, J. *Acta Crystallogr.* **2009**, *E65*, o1573.

(24) (a) McAdam, C. J.; Morgan, J. L.; Murray, R. E.; Robinson, B. H.; Simpson, J. *Aust. J. Chem.* **2004**, *57*, 525. (b) McAdam, C. J.; Robinson, B. H.; Simpson, J. *Acta Crystallogr.* **2005**, *E61*, m110.

(25) Easton, C. J.; Gulbis, J. M.; Hoskins, B. F.; Scharfbillig, I. M.; Tiekink, E. R. T. *Z. Crystallogr.* **1992**, *199*, 249.

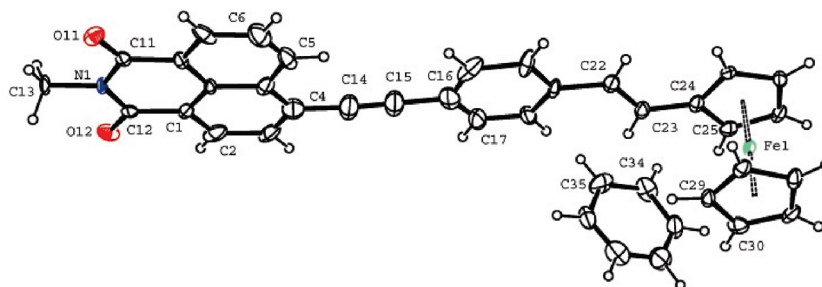


Figure 5. Asymmetric unit of **7** showing the atom-numbering scheme with ellipsoids drawn at the 30% probability level. Only the first two C atoms of consecutively numbered phenyl and cyclopentadienyl rings are numbered. Selected bond distances [Å] and angles [deg]: C4–C14 1.482(9); C14–C15 1.207(14); C15–C16 1.479(16); C19–C22 1.506(11); C22–C23 1.318(12); C23–C24 1.456(11); (C24···C28) ring av C–C 1.42(1); (C29···C33) ring av C–C 1.423(8); Fe1···(C24–C28) av 2.045(7); Fe1···(C29–C33) av 2.044(7); C4–C14–C15 176.1(14); C14–C15–C16 179.6(16); C19–C22–C23 125.6(9); C22–C23–C24 123.7(9).

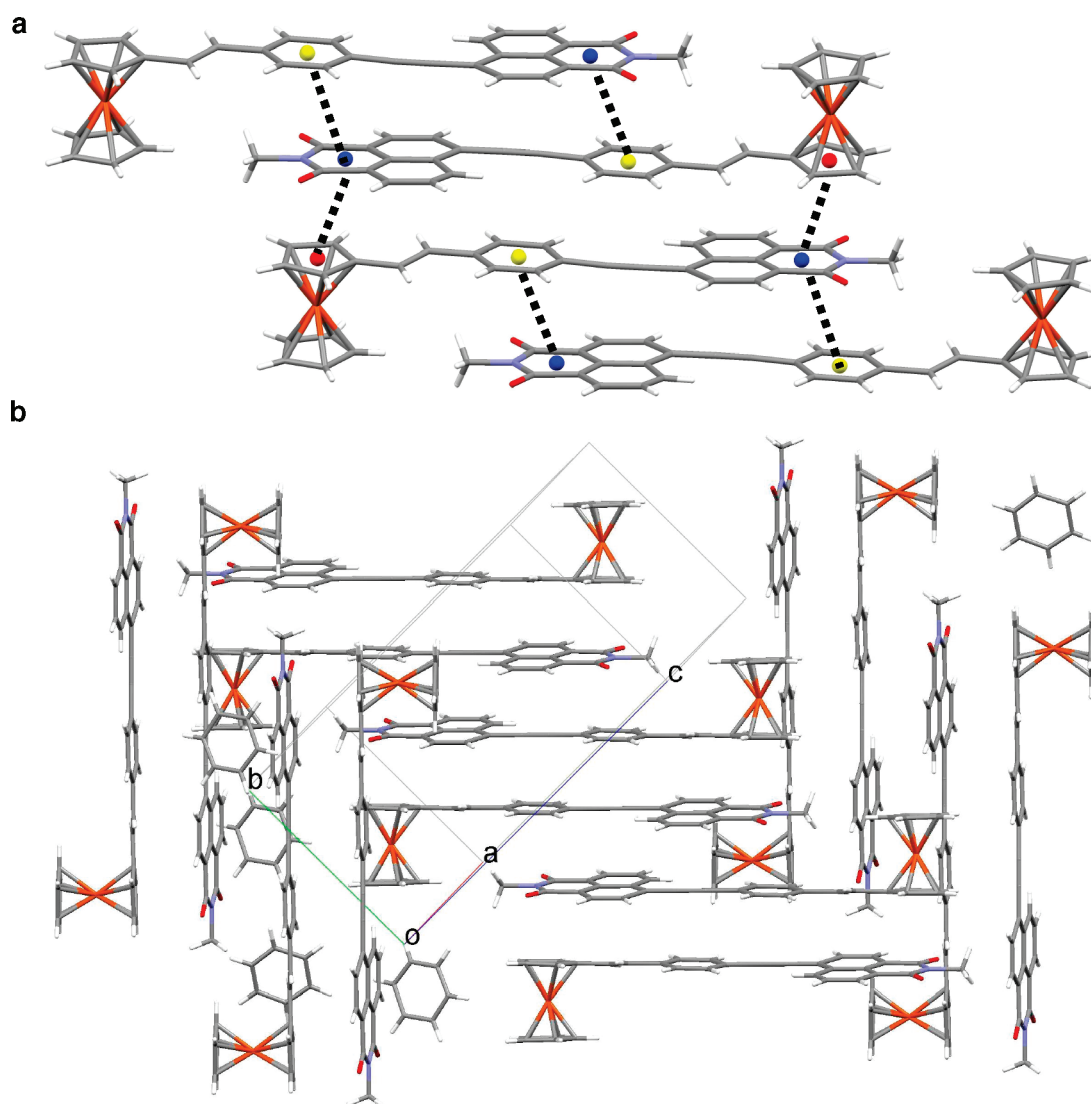


Figure 6. (a) Offset $\pi \cdots \pi$ stacking in **7** with close centroid···centroid interactions shown as dashed lines. (b) Crystal packing in **7**.

In the crystal structure, $\pi \cdots \pi$ stacking interactions between the substituted Cp ring of the ferrocene and the amide ring of an adjacent naphthalimide (Cg1···Cg3 = 3.508(5) Å, symmetry operation $-x, 1-y, -z$) and between the amide ring and the benzene ring of the spacer group (Cg3···Cg4 = 3.705(5) Å, symmetry operation $-x, -y, -z$) form offset

stacks of molecules with the ferrocenyl substituents packing in a head-to-tail fashion at either end of each stack, Figure 6a. Weak C22–H22···O12 hydrogen bonds and C–H··· π interactions involving the benzene solvate molecules link individual molecules in each stack to four adjacent molecules. These in turn stack to generate a series of approximately orthogonal

Table 1. Electrochemical, UV–Vis, and Fluorescence Data for 1–12

compound	$E/V^a(i_{pr}/i_{pt})$			$\lambda_{Abs}(\epsilon)^c$			$\lambda_{Flu}(\Phi_f)^d$
	[Fc] ⁺⁰	[Naph] ^{0/-}	[Ar] ^{0/-}	A ($\pi-\pi^*$)	B ($\pi-\pi^*$)	C	
1 ⁷	0.60 (1.0)	-1.20 (0.5)			391 (13)	526 (5)	
2	0.55 (1.0)			326 (39)		460 (2.2)	
3	0.55 (1.0)			348 (30)		460 (3.3)	
4		-1.06 (0.9)		304 (28)	384 (34)		465 (0.55)
5		-1.09 (0.9)		280 (11)	396 (33)		432 (0.52)
6		-1.07 (0.8)		291 (11)	375 (28)		435 (0.51)
7	0.57 (1.0)	-1.08 (0.9)		282 (13)	390 (25)		
8		-1.07 (0.9)		295 (14)	376 (31)		
9	0.55 (1.0)	-1.08 (1.0)		338 (23)	393 (28)	500 (7.5)	444 (0.002)
10		-1.03 (1.0)	-1.38 (0.8)	352 (23)	390 (31)		
11		-1.0 (0.3)	-1.4 ^b	293 (24)	383 (33)		463 (0.53)
12	0.60 (1.0)	-1.03 (1.0)	-1.33 (0.9)	399 (32)	399 (32)	~500 (3) ^e	471 (0.01)
				342 (29)	390 (35)		
				350 (30)			
				353 (12)	444 (20)		579 (0.03)
				365 (13)	461 (20)		
				353 (12)	447 (21)		581 (0.02)
				370 (12)	470 (21)		
				353 (13)	477 (25)		588 (0.002)
				370 (11)			

^a 1×10^{-3} M in CH₂Cl₂, Pt, 0.1 M TBAPF₆, 20 °C; referenced against decamethylferrocene [Fc*]⁺⁰, for which [FcH]⁺⁰ = 0.55 V;²⁶ i_{pr}/i_{pt} at 100 mV s⁻¹.
^b Irreversible. ^c In CH₂Cl₂; λ nm ($\epsilon/\text{mol}^{-1} \text{cm}^{-1} \text{L} \times 10^3$), 20 °C. ^d In CH₂Cl₂; λ nm, (Φ_f), 20 °C. ^e Under the naphthalimide envelope.

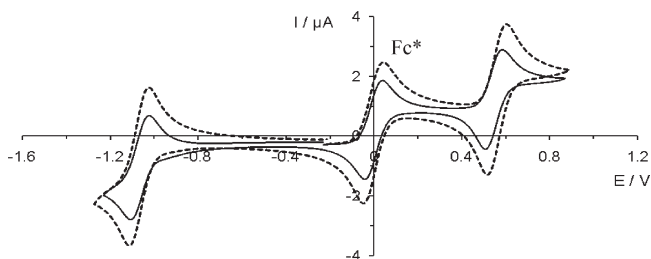


Figure 7. Cyclic voltammograms of 7 (---) and 9 (—) ($\sim 1 \times 10^{-3}$ M in CH₂Cl₂, Pt, 0.1 M TBAPF₆, 100 mV s⁻¹, 20 °C, referenced against [Fc*]⁺⁰, for which [FcH]⁺⁰ = 0.55 V²⁶).

columns in the *bc* plane as a result of similar $\pi \cdots \pi$ stacking interactions, Figure 6b.

Electrochemistry. The results of cyclic voltammetry for compounds 2–12 and the model D–A dyad 1⁷ in dichloromethane solution are shown in Table 1. The ferrocenyl derivatives (2, 3, 7, 9, and 12) display the anticipated chemically reversible [Fc]⁺⁰ couple with $i_{pc}/i_{pa} = 1.0$. Both 2 and 3 show a single reversible wave with $E^0 = 0.55$ V. However for 3, with no interaction between the two equivalent ferrocenyl redox centers, this is a two-electron process. The oxidation potentials for the extended D–S–A systems 7, 9, and 12 with different spacer groups fall in a relatively narrow range, $E^0 = 0.55$ – 0.60 V, Figures 7 and 8. Within experimental error, the potentials of the D–S–A systems are the same as those for the analogous D–S system.⁵ This suggests that augmentation of the simple ferrocenyl–phenyl, –biphenyl, and –anthryl dyads at the 4-, 4'-, and 10-positions, respectively, with an alkyne-linked naphthalimide moiety, has only a minor influence on the [Fc]⁺⁰ couple. The simple D–A dyad 1 has an oxidation potential of 0.60 V.⁷

Reduction processes for several previously reported naphthalimide systems occur with varying degrees of chemical

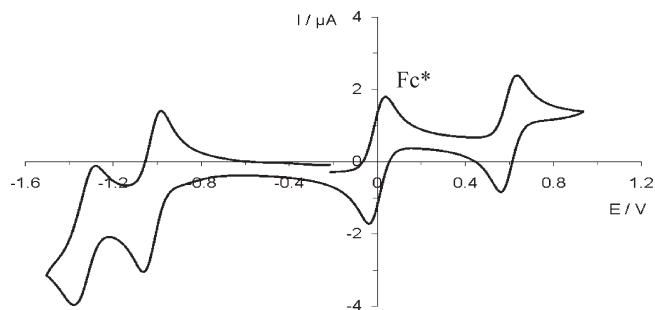


Figure 8. Cyclic voltammogram of 12 (1×10^{-3} M in CH₂Cl₂, Pt, 0.1 M TBAPF₆, 100 mV s⁻¹, 20 °C, referenced against [Fc*]⁺⁰, for which [FcH]⁺⁰ = 0.55 V²⁶).

reversibility and number of electrons involved in the transfer process.^{7,14c,15,27} In this work compounds containing the naphthalimide unit (4–12) show cleanly reversible or quasi reversible one-electron reduction processes in the range -1.03 to -1.09 V (Table 1). With the exception of 11, these processes remain chemically reversible at scan rates in the range 50–500 mV s⁻¹ and can be assigned to a one-electron reduction of the naphthalimide moiety. Predictably, replacement of a phenyl spacer with biphenyl has no effect on the naphthalimide reduction potential. Peak-to-peak separations for both the ferrocenyl oxidation and the naphthalimide reduction resemble that of the internal decamethylferrocene chemical reference, so we can consider the waves Nernstian. Peak current values proportional to $v^{1/2}$ indicate a diffusion-controlled process. For S–A and D–S–A compounds incorporating an anthryl group a subtle (~ 50 mV) anodic shift of the naphthalimide reduction peak occurs, but more importantly, an additional one-electron process at

(26) Barrière, F.; Geiger, W. E. *J. Am. Chem. Soc.* **2006**, *128*, 3980.

(27) (a) Altieri, A.; Gatti, F. G.; Kay, E. R.; Leigh, D. A.; Martel, D.; Paolucci, F.; Slawin, A. M. Z.; Wong, J. K. Y. *J. Am. Chem. Soc.* **2003**, *125*, 8644. (b) Nelsen, S. F. *J. Am. Chem. Soc.* **1967**, *89*, 5925. (c) Sioda, R. E.; Koski, W. S. *J. Am. Chem. Soc.* **1967**, *89*, 475. (d) Ryabinin, V. A.; Starichenko, V. F.; Vorozhtsov, G. N.; Shein, S. M. *Zhur. Struct. Khim.* **1978**, *19*, 804.

−1.33 V is also observed, Figure 8, associated with the anthryl moiety.²⁸ This also appears reversible over a wide range of scan rates. The exception again is **11**, where the electrochemistry is uniformly irreversible. Clearly cleavage following reduction of the reactive 9-iodo substituent is responsible; confirmation of this is provided by comparison with the reversible electrochemical sweeps of D–S–A **12** and the model compound **10**, where the iodine substituent is replaced by hydrogen.

Electronic Spectra. UV–visible data for **2–12** and the model D–A dyad **17** are given in Table 1. For **4–12**, the broad absorption bands of λ_{abs} **A** (280–370 nm) and λ_{abs} **B** (375–477 nm) are assigned to π – π^* transitions of the *p*-band of the aryl group²⁹ and the 1,8-naphthalimide, respectively. Ferrocenyl derivatives **2** and **3** show the aryl spacer absorption **A** at ca. 330 nm, but in the absence of the masking by the strongly absorbing naphthalimide chromophore, we can now observe the weaker ferrocenyl transition **C** at 460 nm. Predictably, these spectral results fit comfortably with findings from previous work on ferrocenyl ethenyl simple polyaromatic dyad systems. Specifically, an ethenyl-connected ferrocenyl results in some perturbation of arene π orbitals, as evidenced by a less-structured and significantly red-shifted **A** (compared with the parent arene) UV *p*-band. Second, the wavelength of the visible spectrum ferrocenyl-based absorption **C** is independent of the simple polyaromatic, but the intensity increases with annulation.⁵ Band **C** for compound **3** with two ferrocenyl chromophores has approximately twice the molar absorptivity of the mono(ethenylferrocenylated) **2**. This finding supports our interpretation of the electrochemistry for **3** that the two metallocene substituents act additively and not cooperatively.

Electronic spectra of **6–9** are shown in Figure 9. Attachment of an ethenyl ferrocene to precursor (X–S–A) compounds **6** and **8** to generate D–S–A dyads **7** and **9** has similar consequences on absorption **A**; the aryl π – π^* transition undergoes a red-shift in comparison to that of the equivalent D–S. The naphthalimide band loses vibrational fine structure and shows only a slight red-shift from X–S–A.

Manifestly different from D–S **2** and **3**, the ferrocenyl absorption of D–S–A **7** is stronger and red-shifted from ca. 460 nm, behavior typical of a strongly conjugated D–A system³⁰ and assignable to metal-to-ligand charge transfer (MLCT)^{4–7,9} with extensive charge separation in the singlet excited state. It occurs at similar intensity but not as low energy as the model ferrocenylethenyl naphthalimide, **17**. Evidence for the inverse distance dependence of the conjugation is provided by the much weaker (masked by the naphthalimide spectral envelope) **C** band of the longer biphenyl, **9**, cf. phenyl spacer, **7**, dyad. Clearly the donor–acceptor interaction propagates through the phenyl spacer (and connective links) and to a lesser extent through the biphenyl system. The **C** absorption for **7** displays the classic solvent effect³¹ characteristic of a charge transfer (CT) band with λ_{abs} shifting to lower energy with increased solvent polarity³² (Supporting

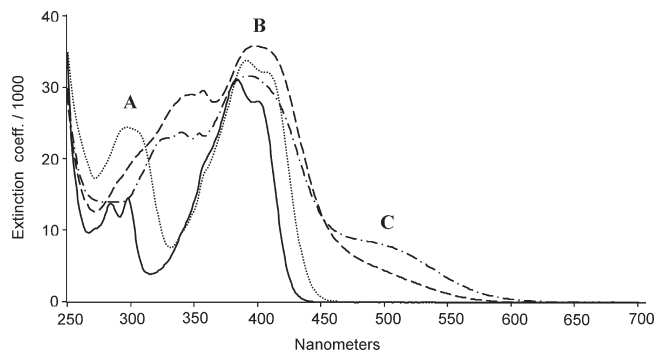


Figure 9. Electronic spectra of **6** (—), **7** (– · –), **8** (····), and **9** (– – –) in CH₂Cl₂.

Information, Figure S3). Determining whether the charge transfer is optical (full charge separation upon excitation) or photoinduced (stepwise, formation of a localized excited state followed by charge separation) will be addressed by time-resolved studies.¹⁹

The electronic spectra for the anthryl systems proved similar (Table 1 and Supporting Information, Figure S4). The model **10** and halo X–S–A precursor **11** again show **A** and **B** structured features attributable to the anthryl and naphthalimide π – π^* transitions. The anthryl band however does not appear to red-shift upon attachment of the ethenylferrocene to produce **12**. Anomalous behavior has been previously noted for ferrocenylethenyl anthracene derivatives,⁵ ascribed to their inability to avoid “fjord”-type interactions³³ and maintain coplanarity (and hence conjugation) between the ethenyl and the two anthryl *peri* hydrogens. We would predict an equivalent MLCT band to that observed for **7**, but this feature is either not resolved from or is masked by the naphthalimide’s broad spectral envelope.

Oxidation of the ferrocene groups in **7**, **9**, and **12** causes significant changes to the UV spectra and the growth of additional absorption bands in the near-infrared region. These are the result of a reversal of the ferrocenyl donor role from that of the ferrocenium acceptor. The resultant low-energy ligand-to-metal charge transfer (LMCT) has been presented for ferrocenyl naphthalimide dyads previously,^{7,8} but closer examination has revealed a second lower energy transition again. Details of this, together with TD-DFT calculations and the results of time-resolved studies on these and related molecules, will be reported in another publication.¹⁹

Emission Spectra. Fluorescence data for **4–12** are given in Table 1. The emission spectra are approximate mirror images of their long-wavelength absorption spectra, a result commonly encountered for rigid polyaromatic systems and indicative of the geometry of the molecule in its relaxed Franck–Condon excited state being not very different from that of the ground state molecule. The absorption and emission spectra of **8** and **9** in CH₂Cl₂ are shown in the Supporting Information, Figure S5. As with the absorption bands, the biphenyl derivatives **4**, **8**, and **9** display emission bands at lower energy than their phenyl equivalents **5–7**; the anthryl compounds **10–12** are at lower energy again. This behavior is predicted from that of the simple aromatics themselves.²⁹ As expected, in all cases, attachment of a ferrocenyl substituent to an S–A fragment to generate the D–S–A systems

(28) (a) Rosa-Montañez, M. E.; Jesús-Cardona, H. D.; Cabrera, C. R. *Electrochim. Acta* **1997**, *42*, 1839. (b) Cao, W.; Zhang, X.; Bard, A. J. *J. Electroanal. Chem.* **2004**, *566*, 409.

(29) (a) Jones, R. N. *Chem. Rev.* **1947**, *41*, 353–371. (b) Clar, E. *Polycyclic Hydrocarbons*, Vol. 1; Academic Press: London, 1964.

(30) Barlow, S.; Marder, S. R. *Chem Commun.* **2000**, 1555.

(31) Alexiou, M. S.; Tychoopoulos, V.; Ghorbanian, S.; Tyman, J. H. P.; Brown, R. G.; Brittain, P. I. *J. Chem. Soc., Perkin Trans. 2* **1990**, 837.

(32) Reichardt, C. *Angew. Chem., Int. Ed. Engl.* **1979**, *18*, 98.

(33) Bartle, K. D.; Jones, D. W. *Adv. Org. Chem.* **1972**, *8*, 317.

results in significant intramolecular quenching of the fluorescence.^{7,34} The higher fluorescence quantum yield obtained for the D–S–A with the longer biphenyl spacer **9** (cf. phenyl and anthryl **7** and **12**) supports this mechanism.

Conclusions

Donor–spacer–acceptor compounds consisting of ferrocene as the donor and naphthalimide as the acceptor can be prepared in reasonable yield with the appropriate synthetic strategy. Investigation of the compounds by X-ray crystallography was rather challenging, due to extensive π – π stacking associated with the inherently planar spacer and acceptor naphthalimide moieties, leading to ready aggregation in the solid state and affecting the quality of the crystals. Nonetheless, three crystal structures (**2**, **4**, and **7**) of D–S, S–A, and D–S–A configuration were obtained, which provided insight into the intramolecular and intermolecular spatial arrangements.

The spacers in the D–S–A compounds had minimal effect on the ferrocenyl oxidation potentials and the naphthalimide reduction potentials. While it is common that upon oxidation of the ferrocenyl unit, a chemically reversible one-electron oxidation process would be obtained, it is less usual that a chemically reversible one-electron reduction process was obtained for the naphthalimide unit.

All D–S–A compounds showed evidence of charge transfer. Oxidation of the ferrocenyl moiety, which resulted in bleaching of the MLCT band and the growth of two new LMCT bands in the near-infrared region, is to be reported on in more detail. As predicted, the fluorescence of all D–S–A compounds was significantly quenched due to the presence of the ferrocene donor.

Experimental Section

Solvents were dried and distilled by standard procedures, and unless otherwise stated all reactions were performed under nitrogen. Microanalyses were carried out by the Campbell Microanalytical Laboratory, University of Otago. Mass spectra were recorded on a Shimadzu LCMS-QP8000 and a Bruker micrOTOF. IR spectra were recorded on a Perkin-Elmer Spectrum BX FT-IR spectrometer. ¹H and ¹³C NMR spectra were recorded on Varian Unity Inova 300 and 500 MHz spectrometers in CDCl₃ (7.26 ppm) at 25 °C. Electronic spectra were recorded on a Varian Cary 500 UV–vis spectrophotometer. Fluorescence measurements were conducted on optically dilute samples (absorbance < 0.05) in spectroscopic grade solvents, and the quantum yield was calculated by comparing the integrated fluorescence spectra with a comparable compound, fluorescein ($\Phi_F = 0.94$).³⁵ The estimated error in the determination of Φ_F was 20%. Cyclic and square-wave voltammetry in CH₂Cl₂ were performed using a three-electrode cell with a polished Pt 1 mm disk working electrode; solutions were $\sim 10^{-3}$ M in electroactive material and 0.10 M in supporting electrolyte (recrystallized TBAPF₆). Data were recorded on a Powerlab/4sp computer-controlled potentiostat. Scan rates of 50–500 mV s⁻¹ were typically employed for cyclic voltammetry. All potentials are referenced to decamethylferrocene; $E_{1/2}$ for sublimed ferrocene was 0.55 V.³⁶

Ethenylferrocene,³⁷ 4-ethynyl-*N*-methyl-1,8-naphthalimide,^{24a} and 9,10-diiodoanthracene³⁸ were prepared by published or modified literature methods. Other compounds were purchased from Aldrich and used as received.

(E)-4-Bromo-4'-(ethenylferrocenyl)biphenyl (2). Ethenylferrocene (0.64 g, 3.00 mmol), 4,4'-dibromobiphenyl (0.94 g, 3.00 mmol), tri-*o*-tolylphosphine (0.27 g, 0.90 mmol), Pd^{II} acetate (0.20 g, 0.90 mmol), and 6 mL of NEt₃ were heated at 80 °C in 60 mL of DMF for 24 h. Solvent was removed *in vacuo* and the residue purified by column chromatography (SiO₂, CH₂Cl₂/hexane, 1:5) to give the second band, from which orange crystals of **1** were obtained on removal of solvent, 0.15 g (11%). Anal. Calcd for C₂₄H₁₉FeBr: C 64.05, H 4.32. Found: C 64.07, H 4.22. APCI-APCI-MS: 445 (MH)⁺. ¹H NMR (δ): 4.15 (s, 5H, C₅H₅), 4.30 (t, 2H, Fc-H _{β}), 4.48 (t, 2H, Fc-H _{α}), 6.73 {d ($J = 16$ Hz), Fc-CH=}, 6.93 {d ($J = 16$ Hz), =CH-biph}, 7.52 (m, 8H, biph. H). IR (KBr): 960 (*E*-CH=CH wag) cm⁻¹.

(E,E)-4,4'-Bis(ethenylferrocenyl)biphenyl (3). Following elution of **2**, the fourth band from the above column gave an orange solid of **3** upon removal of solvent, 0.38 g (22%). Anal. Calcd for C₃₆H₃₀Fe₂: C 75.29, H 5.26. Found: C 75.38, H 5.54. APCI-MS: 575 (MH)⁺. ¹H NMR (δ): 4.16 (s, 10H, C₅H₅), 4.31 (s, 4H, Fc-H _{β}), 4.50 (s, 4H, Fc-H _{α}), 6.73 {d ($J = 16$ Hz), Fc-CH=}, 6.92 {d ($J = 16$ Hz), =CH-biph}, 7.50 {d ($J = 8$ Hz), 4H, biph. H}, 7.59 {d ($J = 8$ Hz), 4H, biph. H}. IR (KBr): 959 (*E*-CH=CH wag) cm⁻¹.

4-Ethynyl-4'-(4-ethynyl-*N*-methyl-1,8-naphthalimide)biphenyl (4). 4,4'-Diethynylbiphenyl (0.61 g, 3.00 mmol) and 4-bromo-*N*-methyl-1,8-naphthalimide (0.59 g, 2.00 mmol) were added to 50 mL of degassed ^tPr₂NH containing 2% CuI and 2% PdCl₂(PPh₃)₂. The resulting cloudy yellow suspension was heated to reflux for 2 h and stirred overnight at room temperature. Solvent was removed *in vacuo* and the residue purified by column chromatography (SiO₂, CH₂Cl₂). The second band eluted yielded a sulfur yellow solid, **3**, 0.35 g (43%). Anal. Calcd for C₂₉H₁₇NO₂: C 84.65, H 4.16, N 3.40. Found: C 84.47, H 4.14, N 3.34. ESI-MS: 434.11 [calcd (M + Na)⁺ 434.12]. ¹H NMR (δ): 3.17 (s, 1H, C \equiv CH), 3.58 (s, 3H, N-CH₃), 7.61 (s, 4H, biph. H), 7.67 {d ($J = 8$ Hz), 2H, biph. H}, 7.76 {d ($J = 8$ Hz), 2H, biph. H}, 7.87 {dd ($J = 8, 7$ Hz), naphth. H₆}, 7.99 {d ($J = 8$ Hz), naphth. H₃}, 8.59 {d ($J = 8$ Hz), naphth. H₂}, 8.68 {dd ($J = 7, 1$ Hz), naphth. H₇}, 8.77 {dd ($J = 8, 1$ Hz), naphth. H₅}. IR (KBr): $\nu_{C\equiv C}$ 2194, $\nu_{C=O}$ 1691, 1651 cm⁻¹.

(4-Ethynyl-*N*-methyl-1,8-naphthalimide)benzene (5). 4-Ethynyl-*N*-methyl-1,8-naphthalimide (0.20 g, 0.85 mmol) and 1-iodobenzene (0.19 mL, 1.70 mmol) were added to 25 mL of degassed ^tPr₂NH containing 2% CuI and 2% PdCl₂(PPh₃)₂. The resulting brown mixture was heated to reflux for 7 h. Solvent was removed *in vacuo* and the residue purified by column chromatography (SiO₂, CH₂Cl₂), from which the second band yielded a yellow solid, 0.19 g (72%). Anal. Calcd for C₂₁H₁₃NO₂: C 81.01, H 4.21, N 4.50. Found: C 81.08, H 4.27, N 4.53. APCI-MS: 312 (MH)⁺. ¹H NMR (δ): 3.56 (s, 3H, N-CH₃), 7.44 {t ($J = 3$ Hz), ph. H₁₈, H₁₉, and H₂₀}, 7.67 (m, 2H, ph. H₁₇ and H₂₁), 7.82 {t ($J = 8$ Hz), naphth. H₆}, 7.93 {d ($J = 8$ Hz), naphth. H₃}, 8.54 {d ($J = 8$ Hz), naphth. H₂}, 8.63 {d ($J = 7$ Hz), naphth. H₇}, 8.71 {d ($J = 8$ Hz), naphth. H₅}. IR (KBr): $\nu_{C\equiv C}$ 2204, $\nu_{C=O}$ 1700, 1666 cm⁻¹.

1-Bromo-4-(4-ethynyl-*N*-methyl-1,8-naphthalimide)benzene (6). 4-Ethynyl-*N*-methyl-1,8-naphthalimide (0.66 g, 2.81 mmol) and 1,4-dibromobenzene (0.66 g, 2.81 mmol) were added to 50 mL of degassed ^tPr₂NH containing 2% CuI and 2% PdCl₂(PPh₃)₂. The resulting black mixture was heated to reflux for 16 h. Solvent was removed *in vacuo* and the residue purified by column chromatography (SiO₂, CH₂Cl₂), giving a second band, which yielded a yellow solid, **6**, 0.26 g (24%). Anal. Calcd for C₂₁H₁₂BrNO₂: C 64.64, H 3.10, N 3.59, Br 20.48. Found: C 64.91,

(34) Fery-Forgues, S.; Delavaux-Nicot, B. *J. Photochem. Photobiol. A* **2000**, *132*, 137.

(35) Magde, D.; Wong, R.; Seybold, P. G. *Photochem. Photobiol.* **2002**, *75*, 327.

(36) Noviadri, I.; Brown, K. N.; Fleming, D. S.; Gulyas, P. T.; Lay, P. A.; Masters, A. F.; Phillips, L. *J. Phys. Chem. B* **1999**, *103*, 6713.

(37) Liu, W.-Y.; Xu, Q.-H.; Ma, Y.-X.; Liang, Y.-M.; Dong, N.-L.; Guan, D.-P. *J. Organomet. Chem.* **2001**, *625*, 128.

(38) Duerr, B. F.; Chung, Y. S.; Czarnik, A. W. *J. Org. Chem.* **1988**, *53*, 2120.

H 3.14, N 3.42, Br 20.57. EI-MS: 389.01 [calcd M^+ ($C_{21}H_{12}^{79}BrNO_2$) 389.01], 391.00 [calcd M^+ ($C_{21}H_{12}^{81}BrNO_2$) 391.00]. 1H NMR (δ): 3.57 (s, 3H, N-CH₃), 7.53 {d ($J = 9$ Hz), ph. H17 and H21}, 7.58 {d ($J = 9$ Hz), ph. H18 and H20}, 7.84 {dd ($J = 9, 7$ Hz), naphth. H6}, 7.95 {d ($J = 8$ Hz), naphth. H3}, 8.57 {d ($J = 8$ Hz), naphth. H2}, 8.66 {dd ($J = 7, 1$ Hz), naphth. H7}, 8.70 {dd ($J = 9, 1$ Hz), naphth. H5}. IR (KBr): $\nu_{C=C}$ 2207, $\nu_{C=O}$ 1699, 1661 cm^{-1} .

(E)-1-Ethenylferrocenyl-4-(4-ethynyl-N-methyl-1,8-naphthalimide)benzene (7). **6** (0.21 g, 0.54 mmol), ethenylferrocene (0.23 g, 1.08 mmol), tri-*o*-tolylphosphine (0.04 g, 0.16 mmol), Pd^{II} acetate (0.04 g, 0.16 mmol), and 2 mL of NEt₃ were heated at 80 °C in 25 mL of DMF for 18 h. Solvent was removed *in vacuo*, and the residue was purified by column chromatography (SiO₂, CH₂Cl₂). The second band eluted yielded a red solid, **7**, 0.13 g (46%). Anal. Calcd for C₃₃H₂₃FeNO₂: C 76.02, H 4.45, N 2.69. Found: C 76.32, H 4.67, N 2.74. EI-MS: 521.11 [calcd M^+ ($C_{33}H_{23}^{56}FeNO_2$) 521.11]. 1H NMR (δ): 3.58 (s, 3H, N-CH₃), 4.17 (s, 5H, C₅H₅), 4.34 (s, 2H, Fc-H _{β}), 4.50 (s, 2H, Fc-H _{α}), 6.72 {d ($J = 17$ Hz), Fc-CH=}, 6.99 {d ($J = 17$ Hz), =CH-ph}, 7.49 {d ($J = 9$ Hz), ph. H18 and H20}, 7.63 {d ($J = 9$ Hz), ph. H17 and H21}, 7.85 {t ($J = 8$ Hz), naphth. H6}, 7.96 {d ($J = 8$ Hz), naphth. H3}, 8.58 {d ($J = 8$ Hz), naphth. H2}, 8.67 {d ($J = 7$ Hz), naphth. H7}, 8.76 {d ($J = 8$ Hz), naphth. H5}. IR (KBr): $\nu_{C=C}$ 2202, $\nu_{C=O}$ 1695, 1655, (E-CH=CH wag) 960 cm^{-1} .

4-Bromo-4'-(4-ethynyl-N-methyl-1,8-naphthalimide)biphenyl (8). 4-Ethynyl-N-methyl-1,8-naphthalimide (0.14 g, 0.60 mmol) and 4,4'-dibromobiphenyl (0.19 g, 0.60 mmol) were added to 25 mL of degassed ¹Pr₂NH containing 2% CuI and 2% PdCl₂(PPh₃)₂. The resulting black mixture was heated to reflux for 3 h. Solvent was removed *in vacuo* and the residue purified by column chromatography (SiO₂, CH₂Cl₂), giving a second band, which yielded a sulfur yellow solid, **8**, 0.07 g (25%). Anal. Calcd for C₂₇H₁₆BrNO₂: C 69.54, H 3.46, N 3.00, Br 17.13. Found: C 69.76, H 3.41, N 3.05, Br 17.10. EI-MS: 465.04 [calcd M^+ ($C_{27}H_{16}^{79}BrNO_2$) 465.04]. 1H NMR (δ): 3.57 (s, 3H, N-CH₃), 7.50 {d ($J = 9$ Hz), biph. H23 and H27}, 7.60 {d ($J = 9$ Hz), biph. H24 and H26}, 7.63 {d ($J = 9$ Hz), biph. H18 and H20}, 7.74 {d ($J = 9$ Hz), biph. H17 and H21}, 7.85 {dd ($J = 9, 8$ Hz), naphth. H6}, 7.97 {d ($J = 8$ Hz), naphth. H3}, 8.58 {d ($J = 8$ Hz), naphth. H2}, 8.66 {dd ($J = 8, 1$ Hz), naphth. H7}, 8.75 {dd ($J = 9, 1$ Hz), naphth. H5}. IR (KBr): $\nu_{C=C}$ 2207, $\nu_{C=O}$ 1697, 1667 cm^{-1} .

(E)-4-Ethenylferrocenyl-4'-(4-ethynyl-N-methyl-1,8-naphthalimide)biphenyl (9). **8** (0.07 g, 0.15 mmol), ethenylferrocene (0.06 g, 0.30 mmol), tri-*o*-tolylphosphine (0.01 g, 0.05 mmol), Pd^{II} acetate (0.01 g, 0.05 mmol), and 0.7 mL of NEt₃ were heated at 80 °C in 25 mL of DMF for 24 h. Solvent was removed *in vacuo* and the residue purified by column chromatography (SiO₂, CH₂Cl₂/pet ether, 1:0.5). The second band eluted yielded an orange solid, **9**, 0.01 g (11%). Anal. Calcd for C₃₉H₂₇FeNO₂: C 78.40, H 4.56, N 2.34. Found: C 78.29, H 4.55, N 2.71. EI-MS: 597.14 [calcd M^+ ($C_{39}H_{27}^{56}FeNO_2$) 597.14]. 1H NMR (δ): 3.58 (s, 3H, N-Me), 4.49 (s, 5H, C₅H₅), 4.77 (s, 2H, Fc-H _{β}), 4.98 (s, 2H, Fc-H _{α}), 6.38 (s, 1H, Fc-CH=), 6.83 (s, 1H, =CH-naphth), 7.60 (m, 8H, biph-H), 7.86 {dd ($J = 8$), naphth H6}, 7.98 {d ($J = 8$ Hz), naphth H3}, 8.59 {d ($J = 8$ Hz), naphth H2}, 8.67 {d ($J = 7$ Hz), naphth H7}, 8.77 {d ($J = 8$ Hz), naphth H5}. IR (KBr): $\nu_{C=C}$ 2203, $\nu_{C=O}$ 1698, 1656, (E-CH=CH wag) 957 cm^{-1} .

9-(4-Ethynyl-N-methyl-1,8-naphthalimide)anthracene (10). 4-Ethynyl-N-methyl-1,8-naphthalimide (0.35 g, 1.48 mmol) and 9-bromoanthracene (0.57 g, 2.22 mmol) were added to 25 mL of degassed ¹Pr₂NH containing 2% CuI and 2% PdCl₂(PPh₃)₂. The mixture was heated to reflux for 10 h. Solvent was removed *in vacuo* and the residue purified by column chromatography (SiO₂, CH₂Cl₂), from which the fourth band yielded an orange solid (0.32 g, 53%). Anal. Calcd for C₂₉H₁₇NO₂: C 84.65, H 4.16, N 3.40. Found: C 84.42, H 4.19, N 3.33. 1H NMR (δ): 3.60 (s, 3H, N-CH₃), 7.58 (m, 2H, anthr. H), 7.68 (m, 2H, anthr. H), 7.90 {dd ($J = 9, 7$ Hz), naphth. H6}, 8.08 {d ($J = 9$ Hz), anthr. H}, 8.18 {d ($J = 8$ Hz), naphth. H3}, 8.54 (s, 1H, anthr. H), 8.63

Table 2. Crystal and Structure Refinement Data for **2**, **4**, and **7**

	2	4	7
emp formula	C ₂₄ H ₁₉ FeBr	C ₂₉ H ₁₇ NO ₂	C ₃₃ H ₂₃ FeNO ₂
fw	443.15	411.44	599.48
temp/K	85(2)	85(2)	85(2)
cryst syst	monoclinic	orthorhombic	monoclinic
space group	<i>P</i> 2 ₁	<i>Pbca</i>	<i>P</i> 2 ₁ / <i>n</i>
<i>a</i> /Å	6.0896(2)	9.5527(2)	16.275(5)
<i>b</i> /Å	7.8142(2)	18.1790(4)	9.665(5)
<i>c</i> /Å	18.7986(6)	23.3617(4)	18.385(5)
β /deg	95.268(2)	90	99.922(5)
<i>V</i> /Å ³	890.76(5)	4056.96(14)	2848.7(19)
<i>Z</i>	2	8	4
μ/mm^{-1}	3.094	0.085	0.567
reflms measd	16 393	66 069	20 104
unique reflms	3517	3990	4120
<i>R</i> _{int}	0.0277	0.0301	0.0741
max. and min. transnm	0.857 and 0.599	0.980 and 0.887	1.000 and 0.699
data/restraints/params	3517/1/254	3990/0/290	4120/52/386
goodness of fit	1.081	1.093	1.184
<i>R</i> [<i>I</i> > 2 σ (<i>I</i>)]	0.0266	0.0411	0.0998
<i>wR</i> (all data)	0.0682	0.1179	0.2514

{d ($J = 8$ Hz), naphth. H2}, 8.69 (m, 3H, anthr. H and naphth. H7}, 8.98 {dd ($J = 8, 2$ Hz), naphth. H5}. IR (KBr): $\nu_{C=C}$ 2183, $\nu_{C=O}$ 1700, 1662 cm^{-1} .

9-Iodo-10-(4-ethynyl-N-methyl-1,8-naphthalimide)anthracene (11). 4-Ethynyl-N-methyl-1,8-naphthalimide (0.18 g, 0.77 mmol) and 9,10-diiodoanthracene (0.33 g, 0.77 mmol) were added to 25 mL of degassed ¹Pr₂NH containing 2% CuI and 2% PdCl₂(PPh₃)₂. The resulting black mixture was heated to reflux for 3 h. Solvent was removed *in vacuo* and the residue purified by column chromatography (SiO₂, CH₂Cl₂), giving a second band, which yielded a red solid, **11**, 0.06 g (15%). Anal. Calcd for C₂₉H₁₆INO₂: C 64.82, H 3.00, N 2.61, I 23.62. Found: C 64.70, H 2.98, N 2.59, I 23.36. EI-MS: 537.02 [calcd M^+ ($C_{29}H_{16}INO_2$) 537.02]. 1H NMR (δ): 3.61 (s, 1H, N-Me), 7.67 (m, 4H, anthr. H), 7.88 {dd ($J = 8$ Hz), naphth. H6}, 8.16 {d ($J = 7$ Hz), naphth. H3}, 8.63 {m, 6H, (anthr. H, naphth. H2 and H7)}, 8.90 {d ($J = 8$ Hz), naphth. H5}. IR (KBr): $\nu_{C=C}$ 2183, $\nu_{C=O}$ 1701, 1663 cm^{-1} .

(E)-9-Ethenylferrocenyl-10-(4-ethynyl-N-methyl-1,8-naphthalimide)anthracene (12). **11** (0.06 g, 0.11 mmol), ethenylferrocene (0.05 g, 0.22 mmol), tri-*o*-tolylphosphine (0.01 g, 0.03 mmol), Pd^{II} acetate (0.01 g, 0.03 mmol), and 0.7 mL of NEt₃ were heated at 80 °C in 20 mL of DMF for 24 h. Solvent was removed *in vacuo* and the residue purified by column chromatography (SiO₂, CH₂Cl₂), giving a second band, which yielded a dark red solid, **12**, 0.04 g (51%). Anal. Calcd for C₄₁H₂₇FeNO₂: C 79.23, H 4.38, N 2.25. Found: C 78.96, H 4.39, N 2.29. EI-MS: 621.14 [calcd M^+ ($C_{41}H_{27}^{56}FeNO_2$) 621.14]. 1H NMR (δ): 3.61 (s, 3H, N-Me), 4.37 (s, 5H, C₅H₅), 4.50 (s, 2H, Fc-H _{β}), 4.75 (s, 2H, Fc-H _{α}), 6.75 {d ($J = 17$ Hz), Fc-CH=}, 7.49 {d ($J = 17$ Hz), =CH-naphth.}, 7.58 {dd ($J = 8$ Hz), 2H, anthr. H}, 7.70 {dd ($J = 9, 7$ Hz), 2H, anthr. H}, 7.91 {dd ($J = 8$ Hz), naphth. H6}, 8.20 {d ($J = 7$ Hz), naphth. H3}, 8.46 {d ($J = 9$ Hz), naphth. H2 and H7}, 8.70 (m, 4H, anthr. H), 9.00 {d ($J = 8$ Hz), naphth. H5}. IR (KBr): $\nu_{C=C}$ 2177, $\nu_{C=O}$ 1693, 1655 cm^{-1} , (E-CH=CH wag) 966 cm^{-1} .

X-ray Data Collection and Structure Solution for **2**, **4**, and **7**. Crystals of **2** (orange plates from CH₂Cl₂/pentane), **4** (yellow plates from CH₂Cl₂/methanol), and **7** (orange plates from CH₂Cl₂/benzene) were used for data collection. Data were collected on a Bruker APEXII CCD diffractometer at 90 K using APEX2³⁹ and processed using SAINT;³⁹ empirical absorption corrections were applied using SADABS.³⁹ Crystal data for the compounds are summarized in Table 2.

(39) APEX2 V2.0-2, SAINT V7.23A, and SADABS 2004/1; Bruker AXS Inc.: Madison, WI, 2006.

The structures were solved using SHELXS⁴⁰ and were refined by full-matrix least-squares on F^2 using SHELXL-97⁴⁰ and Titan2000.⁴¹ All non-hydrogen atoms were assigned anisotropic displacement parameters, with hydrogen atoms included in calculated positions. The alkene C atoms of **2** were disordered over two positions. Refinement of the occupancy factor converged at 0.64(1) for the major disorder component. **2** crystallizes in the non-centrosymmetric space group $P2_1$, and the Flack parameter⁴² $-0.011(9)$ confirms the correct absolute configuration. For **7** a number of high peaks were found in the difference electron density map once all non-hydrogen atoms of the main molecule had been found. These peaks were consistent with the presence of a benzene solvate molecule in the asymmetric unit, and these atoms were included in the final refinements. Additional high peaks in the vicinity of C14 and C15 suggested further possible

(40) Sheldrick, G. M. *Acta Crystallogr., Sect. A* **2008**, *A64*, 112.

(41) Hunter, K. A.; Simpson, J. *TITAN2000: A molecular graphics program to aid structure solution and refinement with the SHELX suite of programs*; University of Otago: New Zealand, 1999.

(42) Flack, H. D. *Acta Crystallogr. Sect. B* **1983**, *B39*, 876.

disorder with an alternative placement of the alkyne unit. However, attempts to generate an appropriate disorder model were not successful. Potential disorder problems also contribute to the relatively high final residuals observed for this structure. The structures of **2**, **4**, and **7** together with the atom labeling are illustrated in Figures 3–5, respectively.

Acknowledgment. We are grateful to the Universiti Malaysia Terengganu for a Ph.D. scholarship to T.T. and the New Zealand Foundation for Research Science and Technology for a postdoctoral fellowship to C.J.M. We also thank the University of Otago for purchase of the diffractometer.

Supporting Information Available: CIF files giving crystallographic data for **2**, **4**, and **7**, crystal-packing diagrams of **2** and **4**, solvent polarity studies for **7**, selected absorption and emission spectra. This material is available free of charge via the Internet at <http://pubs.acs.org>.